Proceedings of the NATO Advanced Research Workshop: Gravitational Wave Data Analysis, edited by B.F. Schutz (Reidel, Dordrecht, 1987).

COMPARISON OF BARS AND INTERFEROMETERS: DETECTION OF TRANSIENT GRAVITATIONAL RADIATION

Daniel Dewey
Massachusetts Institute of Technology
Room 3-253
Cambridge, MA 02139
U.S.A.

ABSTRACT. The signal-to-noise ratios for the detection of transient gravitational radiation are compared for resonant bar and laser interferometric detectors. For the detection of gravitational-wave bursts (e.g., supernovas, particle-black hole interactions), the bar antenna shows its resonant nature with a sensitivity that is broadly peaked near the bar frequency, while the interferometer shows a smooth f^{-1} frequency response (for a fixed gravitational energy emitted in the burst). Applied to the detection of the 'chirp' of radiation emitted in the decay of a compact binary system, the ratio of bar to interferometer sensitivities is independent of the source parameters. Operational bars and interferometers are compared using specific parameters of representative antennas and are seen to be operating near sensitivities allowing Galactic observations. Finally, each detector technology holds promises for increased sensitivity which will allow for collaborative detection of sources as distant as the Virgo cluster.

1.0 INTRODUCTION

The goal of this work is a quantitative comparison of the sensitivites of current and proposed bar and interferometric antennas in well-defined cases in which the antennas are located at a specified distance from and at an optimum orientation to a specified source of gravitational radiation. Using relevant waveforms and antenna models, the signal-to-noise ratios (SNRs) calculated for the antennas can then be directly compared and placed in an astrophysical context. Note that the process of averaging over a variety of parameters (source orientation, antenna orientation, source distance distribution, etc.) and considerations of event rate are left out of this comparison so that interpretation of the results is unambiguous.

As indicated above, the ingredients of the comparison are realistic source and antenna models; these have been presented in detail elsewhere[1] and so here I want to summarize the results and then look to the future which promises higher sensitivities and suggests a collaboration of bar and interferometric antennas. Models of waveforms for transient sources (bursts and chirps) are presented in Section 2; in Section 3 the antenna models are presented and used to calculate the response of each type of antenna to the burst and chirp sources. To enlived the resulting equations, Section 4 presents a comparison of two operational antennas in a Galactic context. Finally in Section 5 the potential of gravity-wave antennas to operate at increased sensitivities is discussed.

2.0 TRANSIENT SOURCE MODELS

2.1. Burst Sources

The expected burst sources consist of stellar collapse events and particle-black hole interactions; examples of predicted wavforms from these sources are given in Fig. 1. These sources can be well modeled[8,9] by a canonical sine burst parameterized by the burst frequency f_g, the burst amplitude h_o, and the number of half-cycles in the burst N_{hc}. The amplitude of these bursts may be realistically set by choosing a distance from source to antenna R and by specifying the total gravitational-wave energy emitted in the burst as ϵMc^2, where M is a mass representative of the system and ϵ is an efficiency for gravity-wave production. This leads to[1]

$$h_o = \frac{1}{R}\left[\epsilon M \frac{4G}{\pi c}\right]^{1/2}\left[N_{hc} f_g\right]^{-1/2} \qquad (2.1)$$

$$\simeq 8\times10^{-18}\cdot\left[\frac{\epsilon M}{10^{-2}M_\odot}\right]^{1/2}\left[\frac{1\ \mathrm{kHz}}{f_g}\right]^{1/2} N_{hc}^{-1/2} \quad .$$

Thus the canonical burst used in this comparison is completely specified by f_g, N_{hc}, ϵM and R.

2.2. Chirp Sources

The chirp of gravitational radiation emitted by a compact binary system as its decays through gravitational radiation has long been considered as a potential source of detectable gravity-waves[10]. The waveform of emitted radiation can be parametrized by the time-until-coalescence τ (Ref.11), in

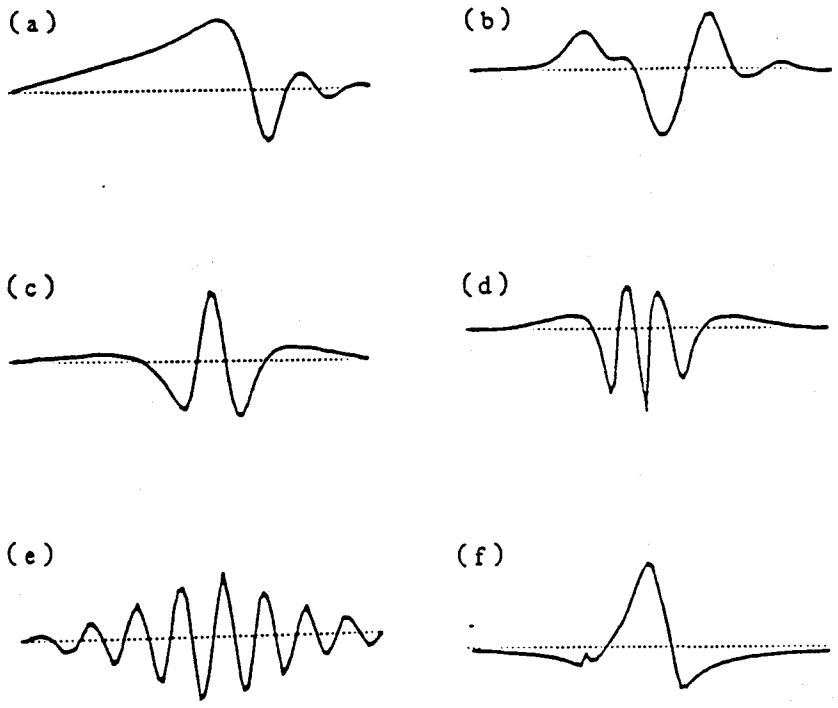

Figure 1. Waveshapes representative of the gravitational radiation expected from burst sources. The waveshapes shown here are digitized versions of published theoretical predictions for a variety of systems: (a) a test particle falling radially into a Schwarzschild black hole (Ref.2), (b) rotating stellar collapse (Ref.3), (c) a test particle scattered from a Kerr black hole (Ref.4), (d) a test particle scattered from a Schwarzschild black hole (Ref.5), (e) damped ellipsoidal stellar collapse (Ref.6), and (f) cold rotating stellar collapse (Ref.7).

terms of which the amplitude, frequency, and phase-remaining-until-coalescence are given by

$$h_{amp}(\tau) = \frac{1}{R} \left[\frac{5G^5}{c^{11}}\right]^{1/4} F^{3/4} \tau^{-1/4} , \qquad (2.2)$$

$$f_g(\tau) = \frac{1}{\pi} \left[\frac{256}{5} \frac{G^{5/3}}{c^5}\right]^{-3/8} F^{-3/8} \tau^{-3/8} , \qquad (2.3)$$

and

$$\phi(\tau) = \frac{16}{5}\left[\frac{256}{5}\frac{G^{5/3}}{c^5}\right]^{-3/8} F^{-3/8}\,\tau^{5/8} \quad , \tag{2.4}$$

where

$$F \equiv \frac{m_1 m_2}{(m_1+m_2)^{1/3}} = \mu(m_1+m_2)^{2/3} = \mu m_T^{2/3} \quad . \tag{2.5}$$

(Equation (2.2) above assumes a source oriented with its angular momentum vector aligned along the observer's line-of-sight.) Because the source parameters m_1 and m_2 appear in both Eq. (2.2) and Eq. (2.3) through the one combination F, an observation of a chirp, i.e., $f_g(\tau)$ and $h_{amp}(\tau)$, allows a determination of both F and R; thus chirp observations will lead to independent distance determinations[12].

The chirp waveform and its second time derrivative which will be used in evaluating the interferometric and bar antenna responses are thus given by

$$h(\tau) = h_{amp}(\tau)\sin[\phi(\tau)+\phi_{arb}] \tag{2.6}$$

$$\ddot{h}(\tau) = -h_{amp}(\tau)\omega_g^2(\tau)\sin[\phi(\tau)+\phi_{arb}] \quad ,$$

and no amplitude or efficiency assumptions are required. An example of $\ddot{h}(t)$ for a chirp waveform is seen in the lower trace of Fig. 2. The wave shape given by Eq. (2.6) is adequate for purposes of comparison, however a variety of corrections may be important in predicting real waveforms[13]. In addition to these corrections the finite size of the radiating objects will lead to deviation from these equations when the separation approaches a few object-radii. For a system of two 1.4 $M_\odot$ neutron stars this will occur when of order five cycles remain in the chirp waveform (i.e., $\phi(\tau)=5\cdot 2\pi$).

3.0 ANTENNA MODELS

The response of both bar and interferometric antennas can be presented in one framework[14]; however, present antenna types each have their own limiting noise sources and data analysis algorithms. Thus, a realistic comparison must take these into account in calculating a value for the signal-to-noise ratio (SNR) for detecting a given source waveform. The antenna models and calculations of SNRs for detecting the burst and chirps of Section 2 are given below.

3.1. Interferometric Antennas

The present limiting noise for interferometric antennas is

the laser shot noise which appears as a white noise of level $\tilde{h}$ in the interferometer output. The gravitational-wave signal h(t) must then be detected in the presence of this noise. The resulting optimal (i.e., maximum) SNR for detection is given by[9,15]

$$(S/N)_I = \frac{1}{\tilde{h}} \left[2 \int h^2(t)\, dt\right]^{1/2} . \qquad (3.1)$$

Note that this SNR is proportional to h(t).

3.1.1 Interferometer response to a burst. For the bursts, substitution of the simple sine-burst waveform into Eq. (3.1) gives the result

$$(S/N)_{I,burst} = \frac{1}{\tilde{h}} \frac{1}{R} \left(\frac{2\epsilon MG}{\pi c}\right)^{1/2} f_g^{-1} , \qquad (3.2)$$

where it is important to recall that this assumes a burst of constant emitted gravitational-wave energy independent of burst frequency.

3.1.2 Interferometer response to a chirp. Because an interferometric antenna typically has a noise spectrum which rises steeply below some minimum frequency f_{min}, the chirp waveform (which extends to the essentially-infinite past) will only be observed when f_g is above f_{min}. Carrying out the integration of Eq. (3.1) from τ given by $f_g(\tau)=f_{min}$ to $\tau=0$ (coalescence) gives, to good approximation, the result

$$(S/N)_{I,chirp} = \frac{1}{\tilde{h}} \frac{1}{R} \frac{\sqrt{5}\, \pi^{-2/3} G^{5/6}}{2\sqrt{2}\, c^{3/2}} F^{1/2} f_{min}^{-2/3} . \qquad (3.3)$$

Note that higher SNR values can be obtained by reducing f_{min} (increasing the total observation time) which has the additional benefit of allowing lower frequency (larger F) chirps to be observed.

3.2. Bar Antennas

Present bar operation seeks to detect a small energy innovation in the presence of a background of thermal and transducer noises[16,17]. With the present signal processing algorithms the detection of a gravity-wave is a two step process: the gravity-wave deposits an amount of energy into the bar then this energy change is detected. This picture assumes that the burst occurs on a time scale short compared to the sample time and the bar ring-down time. The figure

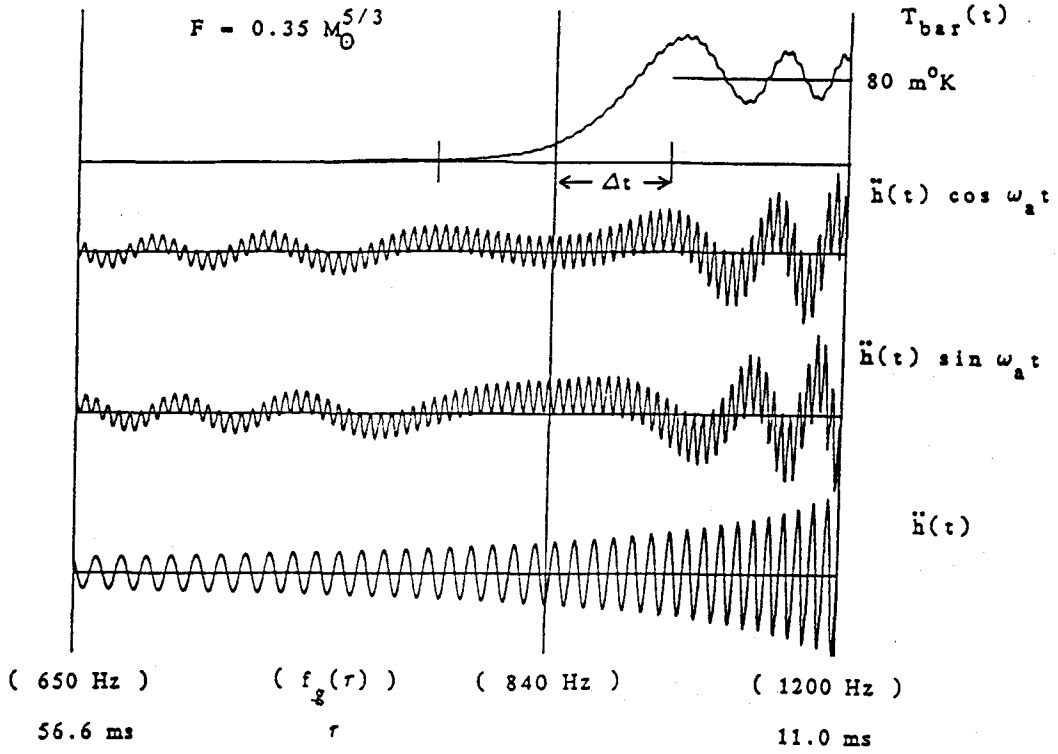

Figure 2. Numerical simulation of a bar antenna's response to a chirp waveform emitted by a compact binary system. Plotted as a function of τ, the time to coalescence, are the $\ddot{h}(t)$ waveform, the integrands of Eq. (3.5), and the temperature equivalent of the energy deposited in the bar as of time τ. The time Δt indicated is calculated from Eq. (3.8) and the asymptotic temperature indicated has been calculated from Eq. (3.4) and Eq. (3.9). This chirp has $F=\mu m_T^{2/3}=0.35$ (two $0.6M_\odot$ objects); for more massive systems the chirp moves to lower frequencies and the number of cycles of the waveform above the (fixed) bar frequency is reduced. Other parameters are as given in Table 1.

of merit for the bar detector, then, is the rms energy noise in the innovation measurement, usually expressed as an equivalent temperature $T_d=E_d/k$. If a source deposits an energy kT_s into the bar, the amplitude signal-to-noise ratio for detection of the source is

$$(S/N)_B = \left[\frac{T_s}{T_d}\right]^{1/2} , \qquad (3.4)$$

and thus the calculation of the SNR for a source requires a calculation of T_s.

In general, T_s can be calculated from the known $\ddot{h}(t)$ waveform and the parameters of the bar using a simple harmonic oscillator model[1]; this leads to

$$(S/N)_B = \frac{1}{T_d^{1/2}} \frac{M_a^{1/2} L_a}{\pi^2 k^{1/2}} \left[\left(\int \ddot{h}(t) \sin\omega_a t \, dt \right)^2 + \left(\int \ddot{h}(t) \cos\omega_a t \, dt \right)^2 \right]^{1/2}, \quad (3.5)$$

where L_a and M_a are the length and mass of the cylindrical bar, $\omega_a (=2\pi f_a)$ is the bar resonant frequency, and the bar is optimally oriented to the strain field. Note that the bracketed term in Eq. (3.5) is just the magnitude of the Fourier amplitude of $\ddot{h}(t)$ at the bar frequency.

3.2.1 Bar response to a burst. For the canonical burst of Section 2.1 evaluation of the integrals of Eq. (3.5) is straight forward (with due care of the delta functions that appear in the second derrivative of h(t)) and gives the result

$$(S/N)_{B,burst} = \frac{1}{T_d^{1/2}} \frac{1}{R} \left(\frac{4\epsilon MG}{\pi kc}\right)^{1/2} L_a (M_a N_{hc} f_g)^{1/2} C\left(\frac{f_a}{f_g}, N_{hc}\right) \quad (3.6)$$

where,

$$C\left(\frac{f_a}{f_g}, N_{hc}\right) = \frac{\sin x}{x} + \frac{\sin y}{y} - \frac{4}{\pi N_{hc}} \cos\left(\frac{f_a}{f_g} \frac{\pi N_{hc}}{2}\right) \quad (3.7)$$

with

$$x = \frac{\pi N_{hc}}{2}\left(1 - \frac{f_a}{f_g}\right)$$

$$y = \frac{\pi N_{hc}}{2}\left(1 + \frac{f_a}{f_g}\right)$$

and upper of 1st and 3rd choices for N_{hc} odd

upper of 2nd choice for $N_{hc} = 1,2,5,6,\ldots$

Note that the function C() is equal to unity when $f_a = f_g$; thus, this tuned response is given by a simple expression (i.e., Eq. (3.6) with C()=1). The off-resonance response of the bar is contained in C(); the width of this essentially reflecting the frequency width of the source.

3.2.2. Bar response to a chirp. Because the bar-chirp interaction is complicated and transient, it is useful to view the interaction numerically to gain insight into the interaction. In Fig. 2 the $\dot{h}$ waveform is shown along with the integrands of Eq. (3.5) and the bar temperature, all plotted as a function of τ, the time-to-coalescence. Of importance here is the finite time-period during which energy is deposited into the bar governed by a near-constant phase relation between the bar frequency and the chirp waveform. This time scale can be calculated[11,1] and at the point in time when the chirp is radiating at f_o it is

$$\Delta t \equiv \text{time until a } \frac{\pi}{2} \text{ phase shift} \tag{3.8}$$

$$= \left[\frac{5\pi^{-8/3}}{192} \frac{c^5}{G^{5/3}} \right]^{1/2} F^{-1/2} f_o^{-11/6}$$

$$\simeq 3 \text{ ms } \left(\frac{F_\odot}{F}\right)^{1/2} \left(\frac{1 \text{ kHz}}{f_o}\right)^{11/6} .$$

Analytic approximations to the integrands of Eq. (3.5) can be made assuming that the chirp waveform has several cycles within the period $\pm\Delta t$ centered on the bar frequency. The result of these calculations is a simple expression giving the bar SNR for detection of a chirp source[1]

$$(S/N)_{B,\text{chirp}} = \frac{1}{T_d^{1/2}} \frac{1}{R} \frac{\sqrt{10}\, G^{5/6}}{\sqrt{3k}\, \pi^{2/3} c^{3/2}} L_a M_a^{1/2} f_a^{5/6} F^{1/2} \tag{3.9}$$

Note that, unlike the interferometer case, decreasing the bar frequency f_a in order to detect lower frequency chirps (larger F values) at face value results in a decrease in the

TABLE 1. List of source and antenna parameters used in the comparisons.

Sources	Bar (4 K)	30-m Interferometer
f_g=100-10kHz	T_d=20 mK	$\tilde{h}=2\cdot10^{-19}$
N_{hc}=4	f_a=840 Hz	f_{min}=500 Hz
$\epsilon M=0.01 M_\odot$	L_a=3.0 m	
R=10kpc	$M_a=4.8\cdot10^3$ kg	
$F=0.35 M_\odot^{5/3}$		

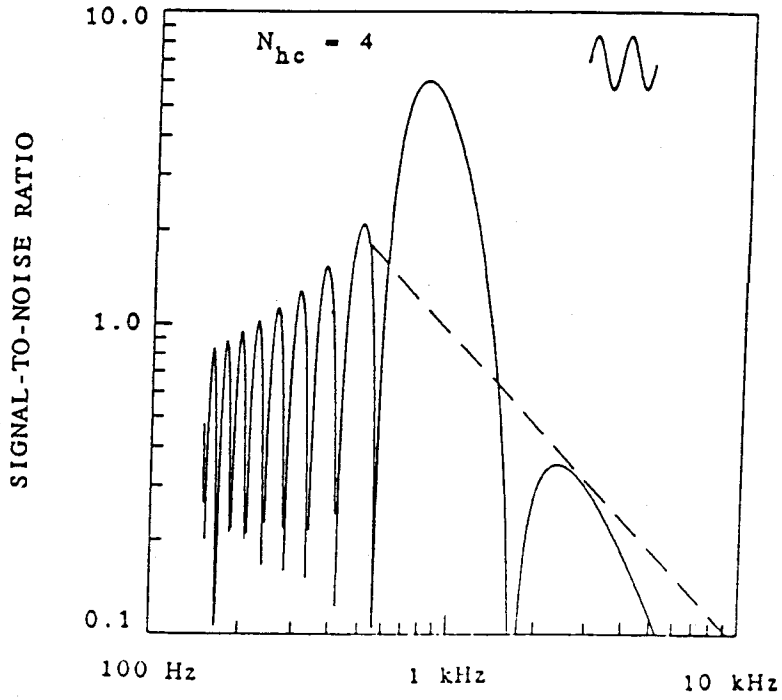

Figure 3. Signal-to-noise ratios (SNRs) for detection of a Galactic burst source as a function of the burst frequency. The 4.2 K Stanford bar SNR is given by the solid curve; the MPQ Garching 30-m interferometer SNR is given by the dashed line. The burst has N_{hc}=4 with a total emitted gravity-wave energy held constant at $10^{-2} M_{\odot} c^2$. The parameters of Table 1 have been used for these calculations.

SNR for chirp detection (with the caveat that changes in L_a and M_a may offset the f_a term).

4.0 COMPARISON FOR TWO OPERATIONAL ANTENNAS

Numerical values of the above equations were calculated using the operational parameters of representative antennas. The parameters used here, Table 1, are those of the Stanford 4 K bar[18] and the MPQ Garching 30-m interferometer[19]; these are well-documented instruments and represent the state-of-the-art as of 1985.

As an example of the resulting comparison for burst source detection Fig. 3 shows the SNR for each antenna as a function of the frequency of the burst which has N_{hc}=4, R=10 kpc (≃Galactic center), and a fairly optimistic efficiency

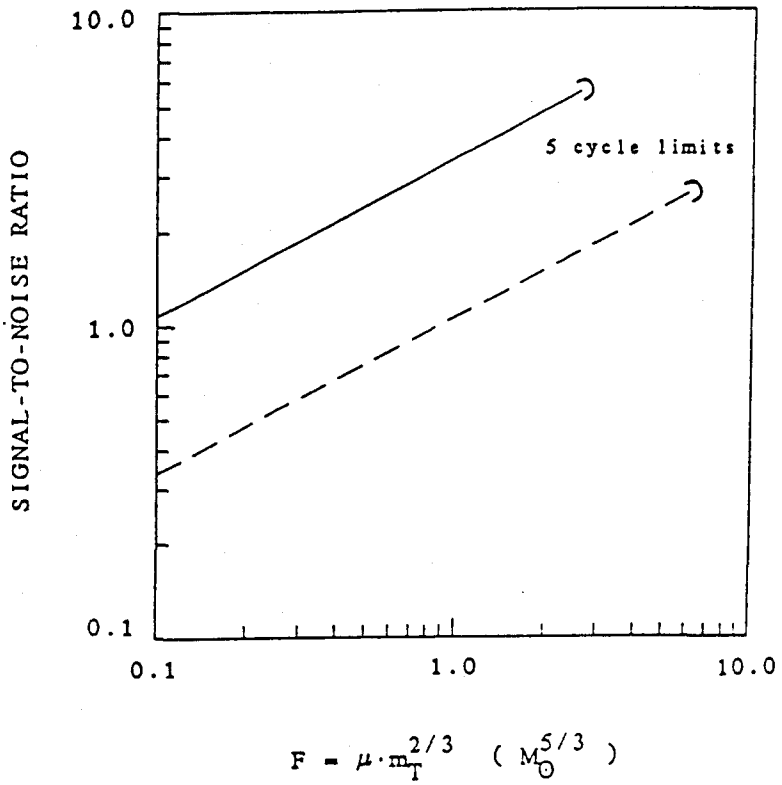

Figure 4. Signal-to-noise ratios (SNRs) for detection of a Galactic chirp source as a function of the source parameter $F=\mu m_T^{2/3}$. The 4.2 K Stanford bar SNR is given by the solid curve; the MPQ Garching 30-m interferometer SNR is given by the dashed line. The curves are discontinued at large F where too few cycles (<5) of the chirp waveform remain for the analytic calculations to be accurate. The parameters of Table 1 have been used for these calculations.

of $\epsilon=0.01$. The bar response shows the frequency dependence of the source given by the C() term in Eq. (3.6). The interferometer curve has been discontinued below 500 Hz where seismic noise dominates.

A comparison of these two antennas when applied to the detection of a chirp is given in Fig. 4 where the SNRs are plotted as a function of the source parameter $F=\mu m_T^{2/3}$. As examination of equations (3.3) and (3.9) shows, both the bar and interferometer have the same dependence on the chirp source parameter F and thus the ratio of bar to interferometer sensitivity is a constant depending only on the instrumental parameters. The curves are shown discontinued at large F values where the chirp source emits too few cycles of waveform at the bar frequency f_a (or above

the interferometer frequency f_{min}) for the results of Eq. (3.9) (or Eq. (3.3)) to be accurate.

5.0 FUTURE SENSITIVITIES AND FUTURE RESEARCH

There are a variety of reasons to develop more sensitive antennas. A higher SNR will allow a transition from simply detecting sources (SNR≃7) to studying source astrophysics (SNR>30). In order to increase the event rate larger volumes of space must be accessible, thus source distances will go from R=10kpc to R>10Mpc. Finally, the efficiency of ϵ=0.01 used in the calculations above is probably optimistic; to ensure detection, sources with ϵ as low as 10^{-6} should be detectable. Thus, sensitivities ten to ten thousand times those of the antennas of Table 1 are desirable. Improvements will come primarilly through reductions in $\tilde{h}$ and T_d as briefly described below[20].

For the interferometric antennas decreases in $\tilde{h}$ depend on increases in the optical storage length Nl (delay-line notation is used for clarity) and in the interferometer input power P, specifically

$$\tilde{h} = \frac{1}{Nl}\,\frac{\lambda}{2\pi}\,\left[\frac{2hc}{\eta P \lambda}\right]^{1/2} \simeq 10^{-19}/\sqrt{Hz}\ \left(\frac{1\ km}{Nl}\right)\frac{1}{\sqrt{P_{Watts}}} \qquad (5.1)$$

where the numerical evaluation has assumed values for λ and η of 514 nm and 0.5 respectively. Going to large baseline antennas will increase Nl from the present ≃3 km to ≃100 kmand reduce the ratio of seismic noise to gravity-wave signal. Improvements in isolation schemes will lower the value of f_{min} improving the SNR for detecting chirp sources. Additional improvements is sensitivity will come through increases in light power P. One promising technique is the recycling[21] of light which leaves the interferometer; this may lead to power increases of order ten or more. More speculative is a reduction in shot noise through squeezing[22], which has, however, produced an increase of a factor of two in equivalent P in recent experiments[23]. Even the quantum limit (determined by the balancing of radiation-pressure noise and shot-noise) will not be accepted with out attemps to circumvent it[24].

For the bar antennas a reduction of T_d may be achieved through reducing the physical temperature of the bar T_a, increasing the bar Q, and through improvements to the transducer system expressed as an increase in the system bandwidth. There are plans to cool the bars to 10-50 mK from the current 4 K, and multi-mode bar systems[25] with increased bandwidth will allow T_d to approach the ideal value of order T_a/Q. Note that with these increased bandwidths, and thus

reduced sample times, the assumption that the gravity-wave deposits energy into the bar on a timescale shorter than the sample time may no longer be valid, especially for chirp sources. Thus, new bar algorithms may be required to optimally detect these events. Finally, with a philosophy similar to squeezed states, back action evasion schemes[26] may improve present systems and allow higher sensitivities than the standard quantum limit would imply.

What kind of sensitivities can we hope to obtain with these improvements? Fig. 5 presents plots of SNR for the *hypothetical* bar and interferometer parameters listed in Table 2. In viewing this figure it is well to adopt the opinion that[27] "mere theoretical notions are ... useless, representing only sterile mental exercises." Even so, this figure does show that each detector technology holds a promise for sensitivities adequate to detect (SNR≃7) sources at Virgo cluster distances and to study (SNR>30) Galactic sources.

This comparison has focussed on transient sources and a comparison for periodic sources needs to be carried out[28]. In the context of transient sources, however, there are a variety of differences between (current) bar and interferometric antennas that have not been addressed; for example: time resolution, non-statistical event rates, antenna patterns, and frequency response. Most of these issues will become important as we analyze systems of many antennas; to this end important ground work on the problem of multiple antenna systems and coincidence rates has been carried out for bar[29] and interferometric[30] systems. In particular it will be important to consider hybrid systems of bars and

TABLE 2. Ficticious antenna systems and their parameters.

	P (W)	N	l (km)	Interferometer Systems
a)	1	2	5	low power, two pass, long arms
b)	10	30	3.3	multi-pass, medium power laser
c)	100	20	5	multi-pass, recycled (×10)

	T_d (K)	f_a (Hz)	M_a (10^3 kg)	L_a (m)	Bar Systems
d)	10^{-4}	800	5.5	3.1	T_a=4 K, three-mode bar
e)	10^{-6}	600	11.0	4.1	T_a=30 mK, multi-mode
f)	$3\cdot10^{-7}$	300	60.0	8.2	T_a=10 mK, massive bar

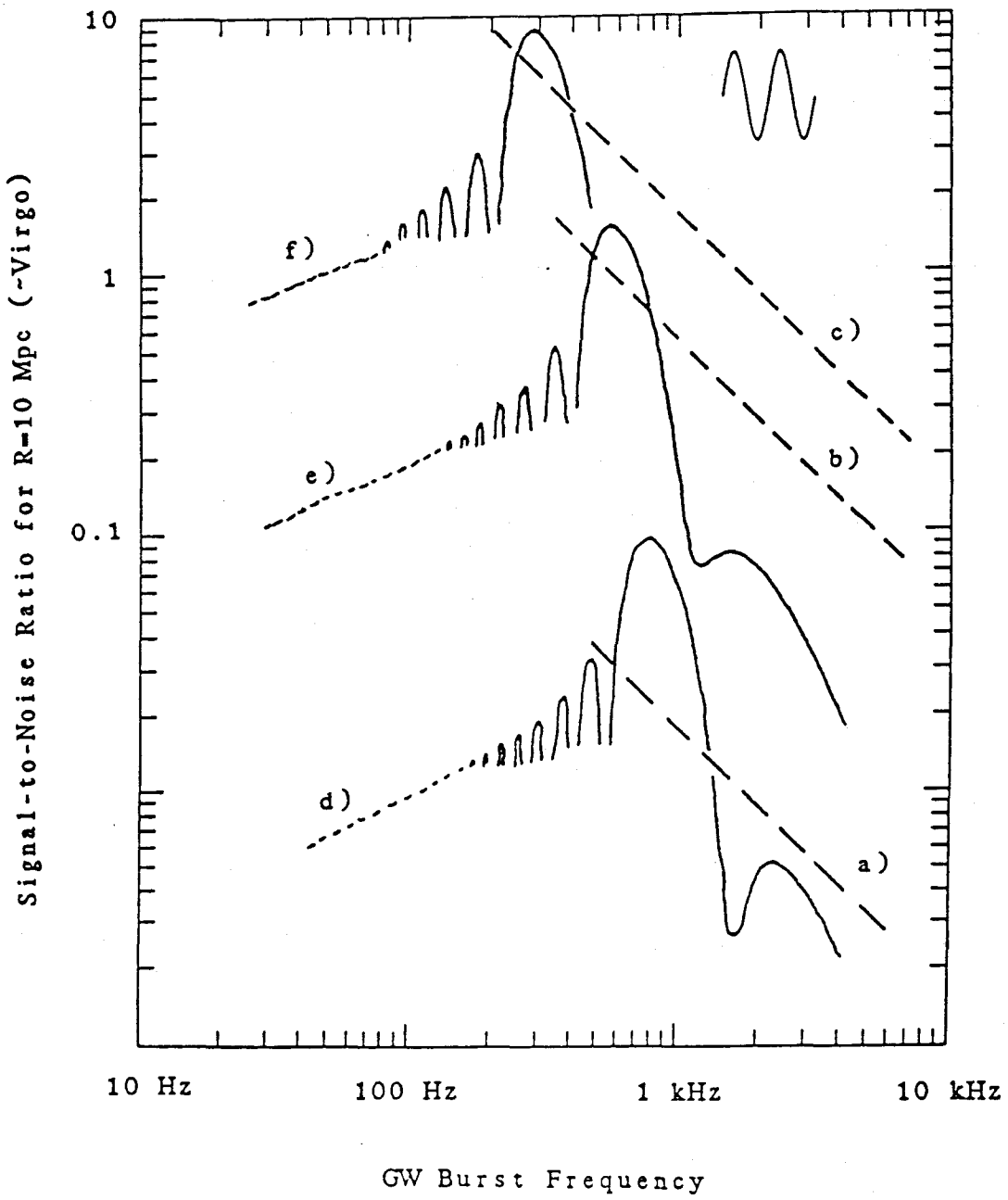

Figure 5. Comparison of *hypothetical* bar and interferometer antennas to a burst source near Virgo (10 Mpc). The bar and interferometer SNRs are plotted as a function of the frequency of the gravity-wave burst; other parameters of the burst are $\epsilon M = 0.01 M_{\odot}$ and $N_{hc} = 4$. The parameters of the ficticious antenna systems are given in Table 2.

interferometers leading to a grand-GRAVNET collaboration in which the antennas work together to detect and study gravitational waves and their astrophysical sources.

ACKNOWLEDGEMENTS

I gratefully acknowledge helpful discussions with W. Johnson, J.P. Richard, P.R. Saulson, and D.H. Shoemaker. This work was supported in part by the National Science Foundation under Grant 85-04836-PHY.

REFERENCES AND NOTES

[1] D. Dewey, scheduled to appear in Phys. Rev. D15, Sept. 15, (1987).
[2] S.L. Detweiler, in *Sources of Gravitational Radiation*, edited by L. Smarr (Cambridge University Press, 1979), p.211.
[3] R.F. Stark and T. Piran, Phys. Rev. Let. 55, 891 (1985).
[4] Y. Kojima and T. Nakamura, Prog. Theor. Phys. 72, 494 (1984).
[5] K. Oohara and T. Nakamura, Prog. Theor. Phys. 71, 91 (1984).
[6] R. Saenz and S. Shapiro, Astrophys. J. 244, 1033 (1981).
[7] R. Saenz and S. Shapiro, Astrophys. J. 221, 286 (1978).
[8] G.W. Gibbons and S.W. Hawking, Phys. Rev. D 4, 2191 (1971).
[9] D. Dewey, in *Proceedings of the Fourth Marcel Grossmann Meeting on General Relativity*, edited by R. Ruffini (Elsevier Science Publishers B.V., Amsterdam, 1986), p.581.
[10] R.L. Forward and D. Berman, Phys. Rev. Let. 18,1071 (1967).
[11] J.P.A. Clark and D.M. Eardley, Astrophys. J. 215, 311 (1977).
[12] B. Schutz, Nature 323, 310 (1986).
[13] A. Krolak, in this volume.
[14] W.H. Press and K.S. Thorne, in *Annual Review of Astronomy and Astrophysics*, edited by L. Goldberg (Anual Reviews Inc., Palo Alto, 1972), p.355.
[15] D. Dewey, "Data Analysis ...", in this volume.
[16] G. Pizzella, in this volume.
[17] P.F. Michelson, J.C. Price, and R.C. Taber, Science 237, 150 (1987).
[18] M. Bassan, W.M. Fairbank, E. Mapoles, M.S. McAshan, P.F. Michelson, B. Moskowitz, K. Ralls, and R.C. Taber, in *Proceedings of the Third Marcel Grossmann Meeting on General Relativity*, edited by H. Ning (North-Holland, Amsterdam, 1983), p.667.
[19] D. Shoemaker, W. Winkler, K. Maischberger, A. Rüdiger,

R. Schilling, and L. Schnupp, in *Proceedings of the Fourth Marcel Grossmann Meeting on General Relativity*, (Ref. 9), p.605.
[20] Many of the contributions to this volume describe planned
[21] detector systems in greater depth than is possible here. Recycling has been demonstrated by the MPQ Garching and Orsay groups as communicated by L. Schnupp and C.N. Man,
[22] respectively, at this workshop.
[23] G. Leuchs, in this volume.
[24] M. Xiao, L. Wu, and H.J. Kimble, Phys. Rev. Lett. **59**, 278 (1987).
[25] Wei-Tou Ni, Phys. Rev. D15 **35**, 3002 (1987).
[26] J.P. Richard, J. Appl. Phys. 60, 3807 (1986).
[27] M.F. Bocko, in this volume.
[28] N.W. Ross, *Three Ways of Asian Wisdom* (Simon and Schuster, New York, 1966), p.94.
Initial examination of the *periodic* sensitivities of bars (Ref. 16) and interferometers shows that in the frequency range where, say, the Stanford bar is operating near the thermal noise limit ($\simeq 840 \pm 5$ Hz) it is two orders of magnitude more sensitive to periodic sources than the MPQ
[29] Garching interferometer!
[30] D. Blair, in this volume.
B.F. Schutz and M. Tinto, Mon. Not. R. astr. Soc. **224**, 131 (1987).